

# Large Liver Cell Dysplasia in Hepatitis B Virus-Related Chronic Liver Disease

Haeryoung Kim

Department of Medicine

The Graduate School, Yonsei University

# Large Liver Cell Dysplasia in Hepatitis B Virus-Related Chronic Liver Disease

Haeryoung Kim

Department of Medicine

The Graduate School, Yonsei University

# Large Liver Cell Dysplasia in Hepatitis B Virus-Related Chronic Liver Disease

Directed by Professor Young Nyun Park

Doctoral Dissertation  
submitted to the Department of Medicine,  
the Graduate School of Yonsei University  
in partial fulfillment of the requirements for the degree of  
Doctor of Philosophy

Haeryoung Kim

June 2008

This certifies that the Doctoral Dissertation  
of Haeryoung Kim is approved.

---

Thesis Supervisor : Young Nyun Park

---

Chanil Park: Thesis Committee Member#1

---

Bong-Kyeong Oh: Thesis Committee Member#2

---

Joo Hang Kim: Thesis Committee Member#3

---

Kwan-Sik Lee: Thesis Committee Member#4

The Graduate School  
Yonsei University

June 2008

## ACKNOWLEDGEMENTS

I would like to begin by expressing my sincerest appreciation to my supervisor Professor Young Nyun Park for her tremendous guidance, encouragement, support and everything else connected to this work. I would also like to express my gratitude to the committee members Professor Chanil Park, Professor Bong-Kyeong Oh, Professor Joo Hang Kim and Professor Kwan-Sik Lee for their enthusiasm, critical review of the manuscript and their valuable comments and advice.

The technical difficulties of this study were very much alleviated thanks to the help of the following colleagues. Jung Hee Lee and Somi Yoon helped with the immunohistochemical staining and senescence-associated- $\beta$ -galactosidase staining. I would also like to recognize Jung Ok Park and Jeong Eun Yoo for their unceasing interest, advice and assistance with the fluorescent in situ hybridization.

I am grateful to the faculty and colleagues of the Department of Pathology, Yonsei University College of Medicine, especially Professor Hoguen Kim, Professor Woo-Ick Yang and Professor Woo-Hee Jung, and also to the faculty of Department of Pathology, Seoul National University Bundang Hospital, for their encouragement and support during the past three years.

Last – and by no means the least – I am very much indebted to my family, including Byung-Min, who have unsparingly granted me their continuous support, both material and spiritual.

Haeryoung Kim

## <TABLE OF CONTENTS>

ABSTRACT.....	1
I. INTRODUCTION.....	4
II. MATERIALS AND METHODS.....	9
A. Patient selection. ....	9
B. Histological examination. ....	9
C. Immunohistochemical stains for markers of cell cycle, proliferation and DNA damage.....	10
D. Quantitative fluorescent in situ hybridization (Q-FISH) for telomere length.....	11
E. Detection of apoptosis: transferase-mediated dUTP-biotin nick end labeling (TUNEL) assay.....	12
F. Senescence-associated- $\beta$ -galactosidase (SA- $\beta$ -Gal) study.....	13
G. Micronuclei index.....	14
H. Statistical analysis... ..	14
III. RESULTS.....	16
A. The prevalence of liver cell dysplasia in HBV-related cirrhosis.....	16
B. Cell cycle checkpoint markers in hepatocarcinogenesis.....	16
C. DNA damage markers in hepatocarcinogenesis.....	19
D. Proliferation and apoptosis in hepatocarcinogenesis.....	22
E. Senescence markers in hepatocarcinogenesis.....	26
IV. DISCUSSION.....	30
V. CONCLUSION.....	36
REFERENCES.....	38
ABSTRACT (IN KOREAN) .....	50

## LIST OF FIGURES

Figure 1. Histopathological features of liver cell dysplasia.....	16
Figure 2. Immunohistochemical stain results for p21.....	17
Figure 3. Scatter plots showing cell cycle checkpoint marker expression.....	19
Figure 4. Immunohistochemical stain of $\gamma$ H2AX foci and micronuclei .....	21
Figure 5. Scatter plots showing frequency of $\gamma$ H2AX foci and micronuclei index .....	22
Figure 6. Scatter plots showing proliferation, apoptosis and net cellular gain .....	25
Figure 7. Results of quantitative FISH for telomere length assessment.....	27
Figure 8. Results of senescence associated- $\beta$ -galactosidase (SA- $\beta$ - gal) study.....	28
Figure 9. Scatter plots showing senescence associated- $\beta$ - galactosidase (SA- $\beta$ -gal) activity .....	29

## LIST OF TABLES

Table 1. Results of cell cycle checkpoint marker labeling index analysis.....	18
Table 2. Results of $\gamma$ H2AX foci and micronuclei index analysis.....	20
Table 3. Results of proliferation and apoptosis index analysis.....	24
Table 4. Results of telomere length analysis.....	26
Table 5. Results of senescence associated- $\beta$ -galactosidase (SA- $\beta$ -gal) activity analysis.....	29

<ABSTRACT>

Large liver cell dysplasia in hepatitis B virus-related chronic liver disease

Haeryoung Kim

*Department of Medicine  
The Graduate School, Yonsei University*

(Directed by Professor Young Nyun Park)

Liver cell dysplasia or dysplastic foci are defined as microscopic lesions measuring less than 1mm in diameter which do not form circumscribed nodules, and are often found in chronic liver disease. These lesions have been classified into two types: large liver cell dysplasia (LLCD) and small liver cell dysplasia (SLCD). Although SLCD has been more or less established as a precursor to hepatocellular carcinoma (HCC), the significance of LLCD is still controversial - while some have favored a reactive/degenerative nature for the lesion, there is increasing evidence that it may actually be related to hepatocarcinogenesis. A comprehensive analysis of LLCD was performed in this study, evaluating the cell cycle dynamics, proliferation and apoptosis, DNA damage and senescence. The molecular features - including senescence, cell cycle checkpoint status, DNA damage and chromosomal instability - and cell dynamics of LLCD in HBV-related cirrhotic livers were explored to further characterize the nature of LLCD.

Thirty-four formalin-fixed specimens and 19 fresh frozen liver specimens were obtained from surgically resected cases of HBV-related cirrhosis and examined for

the presence of LLCD, SLCD and HCC. The immunohistochemical expression of p21, p27, p16, Tp53, PCNA, Ki-67 and  $\gamma$ -H2AX, telomere lengths, apoptotic activity, micronuclei index and senescence-associated  $\beta$ -galactosidase (SA- $\beta$ -Gal) activity were examined for each lesion.

The p21, p27 and p16 cell cycle checkpoint markers - which were expressed at low levels in normal hepatocytes - were activated in cirrhosis but were diminished gradually from LLCD through SLCD to HCC, along with an increase in Tp53 expression. Significant shortening of telomere length was seen in non-dysplastic hepatocytes compared to normal liver, and in LLCD compared to non-dysplastic hepatocytes. There was a general decrease in telomere length from non-dysplastic hepatocytes, LLCD, SLCD to HCC. The accumulation of  $\gamma$ -H2AX foci and the micronuclei index were extremely low in normal hepatocytes and there was a significant gradual increase from non-dysplastic hepatocytes, LLCD, SLCD to HCC. An increase in net cellular gain (high proliferative activity and low apoptotic index) from normal hepatocytes, non-dysplastic hepatocytes, LLCD, SLCD to HCC was seen. The SA- $\beta$ -Gal activity was weaker and less frequent in LLCD compared to the periseptally located non-dysplastic hepatocytes.

The increase in net cellular gain and the weak SA- $\beta$ -Gal activity in LLCD suggest that LLCD may represent a proliferative lesion rather than a population of terminally differentiated end-stage hepatocytes. The loss of cell cycle checkpoint markers in LLCD may allow clonal expansion of hepatocytes with dysfunctional, shortened telomeres, and accumulation of DNA damage and chromosomal instability.

---

Key words : large liver cell dysplasia, hepatocellular carcinoma, hepatitis B virus

# Large liver cell dysplasia in hepatitis B virus-related chronic liver disease

Haeryoung Kim

*Department of Medicine  
The Graduate School, Yonsei University*

(Directed by Professor Young Nyun Park)

## I. INTRODUCTION

Recent advances in imaging diagnosis and an increased awareness of the population for cancer screening has led to growing interest in small hepatic nodules, including early hepatocellular carcinoma (HCC), dysplastic nodules and macroregenerative nodules.<sup>1-7</sup> Liver cell dysplasia (LCD) or dysplastic foci are defined as microscopic lesions measuring less than 1mm in diameter which do not form circumscribed nodules, and have been often found in chronic liver disease.<sup>8,9</sup> These lesions have been classified into two types: large liver cell dysplasia (LLCD) and small liver cell dysplasia (SLCD). SLCD, a lesion first proposed by Watanabe et al. in 1983, is characterized by foci of crowded hepatocytes with high nuclear/cytoplasmic ratio,<sup>10</sup> whereas LLCD is relatively easily recognized under the microscope as foci of cellular enlargement and nuclear pleomorphism, hyperchromasia and multinucleation.<sup>11</sup> Although SLCD has been more or less established as a precursor to HCC,<sup>12,13</sup> the significance of LLCD is still controversial with various studies demonstrating contradictory results. Anthony et al., who coined the term “liver cell dysplasia” (which now corresponds to large liver cell dysplasia) in 1973, found that LLCD was significantly prevalent in hepatitis B virus (HBV)-related cirrhotic livers

harboring HCC and suggested that this lesion was a preneoplastic one.<sup>11</sup> In addition, some studies recognized abnormal DNA contents (aneuploid peaks)<sup>14-19</sup> and numerical chromosomal aberrations<sup>20</sup> in LLCs, and increased net cellular gain in LLC (higher proliferative index and lower apoptotic rates) compared to adjacent hepatocytes,<sup>21</sup> supporting the hypothesis that LLC may be a precursor to HCC. Monoclonality has been found in macronodules with LLC in another study,<sup>22</sup> and follow up studies demonstrated that the presence of the lesion in HBV-related chronic liver disease significantly increased the relative risk of HCC development by 3 to 16-fold<sup>23,24</sup> and that LLC had a high negative predictive value for HCC development.<sup>23</sup> However, others disputed these findings by demonstrating LLC had a low proliferative activity, high apoptotic rate, and no definite histologic continuum to HCC, and suggested that it may simply represent age-related/reactive change of hepatocytes.<sup>25</sup> As there is no consensus yet on the nature of LLC, the pathogenetically non-committal term of “large cell change” instead of “dysplasia” has been recommended as an alternative designation.

The telomere is a TTAGGG-repeat sequence located at the end of the chromosome which is not replicated during the S phase of the cell cycle and hence is shortened with each cell division of somatic cells.<sup>26-29</sup> The telomere stabilizes the chromosomal end from end-to-end fusion, and loss of the telomere leads to repeated breakage-fusion-bridge cycles and the formation of chromosomal instability.<sup>30</sup> The loss of telomere integrity induces a DNA damage response involving the cell cycle checkpoint pathways, leading to replicative senescence (permanent growth arrest, M1 stage). In the absence of functional cell cycle checkpoint pathway responses,

telomeres continue to shorten resulting in crisis (M2 stage).<sup>31,32</sup> Neoplastic cells demonstrate high proliferative activity compared to normal cells, leading to accelerated cell cycles and shorter telomeres, and therefore require reactivation of telomerase before crisis occurs in order to maintain telomere length and gain the ability for indefinite cell proliferation.<sup>31,32</sup> The association between telomere shortening and chromosomal instability has also been demonstrated in HCC: telomeres were significantly shorter in hepatocytes of aneuploid tumors compared to diploid tumors<sup>33</sup> and a correlation was found between telomere shortening and increasing aneuploidy of chromosome 8.<sup>34</sup> Telomerase is an enzyme which adds the telomeric DNA sequence to the 3'-end of eukaryotic cell chromosomes and prevents telomere shortening.<sup>26,27</sup> Significant increases in telomerase activity have been demonstrated in high-grade dysplastic nodules and HCCs compared to cirrhotic nodules and low-grade dysplastic nodules,<sup>35</sup> and telomere length maintenance or even elongation was noted in a substantial number of HCCs compared to corresponding adjacent non-neoplastic livers.<sup>36</sup> Furthermore, high telomerase activity in HCCs was correlated with advanced tumor stage and high chromosomal instability, and poor overall survival was seen in HCCs with high telomerase activity and increased telomere lengths.<sup>36</sup>

The DNA damage response induced by telomere dysfunction involves foci containing  $\gamma$ -H2AX, MRE11, NBS1, MDC1, 53BP1, RAD50 and BRCA1.<sup>28</sup> Of these,  $\gamma$ -H2AX is a phosphorylated histone H2A variant which facilitates DNA damage response by inducing changes in local chromatin structure and by facilitating focal accumulation of DNA-repair and checkpoint proteins to the

damaged regions. It is thus considered to reflect the accumulation of unrepaired DNA damage during aging.<sup>28</sup> Micronuclei are DNA masses similar to small nuclei in the cytoplasm of interphase cells.<sup>37</sup> They arise from acentric chromosome fragments or from whole lagging chromosomes in anaphase or telophase stages, and therefore are regarded as indicators of genomic instability in dividing cells. Micronucleated hepatocytes have been reported to be significantly more frequent in hepatocellular carcinomas compared to cirrhotic regenerative nodules and normal hepatic parenchyma.<sup>38</sup>

Strong arguments indicate that replicative senescence is regarded as a tumor suppressor mechanism that prevents proliferation of genetically unstable precancerous cells, and involves cell cycle checkpoint activation and recruitment of DNA repair foci.<sup>39-42</sup> Therefore, activation of senescence-associated DNA damage checkpoints is present in preneoplastic lesions, but is inactivated during malignant transformation.<sup>41,42</sup>

Cyclin-dependent kinase inhibitors are important regulators of the cell cycle which inhibit unlimited cell growth by regulating the progression from G1 to S phase.<sup>43</sup> There are two types of cyclin-dependent kinase inhibitors, the first being the INK (inhibitor of kinase) family – p16(INK4a), p15(INK4b), p18(INK4c) and p19(INK4d) – and the second being the CIP/KIP (cdk interacting protein/kinase inhibitory protein) family, which include p21(WAF1/CIP1), p27(KIP1) and p57(KIP2). These cell cycle inhibitors have also been utilized as markers of cellular senescence; inactivation of both CIP/KIP and INK pathways have been shown to strongly cooperate in suppressing cellular senescence *in vitro*.<sup>41,42,44</sup> In addition,

senescence-associated  $\beta$ -galactosidase (SA- $\beta$ -Gal), a cytoplasmic enzyme which can be detected at pH 6.0 only in senescent cells,<sup>41,42,45-47</sup> and senescence-associated heterochromatin foci (SAHF) are useful markers of senescence.<sup>42</sup> Recently, other novel markers of senescence have been reported, including the decoy death receptor 2 (DCR2) and the transcription factor differentiated embryo-chondrocyte expressed (DEC1), which have been demonstrated in formalin-fixed tissue sections by immunohistochemistry.<sup>42</sup>

In this study, the molecular features - including senescence, cell cycle checkpoint status, DNA damage and chromosomal instability - and cell dynamics of LLCD in HBV-related cirrhotic livers were explored to further characterize the nature of LLCD.

## II. MATERIALS AND METHODS

### 1. Patient selection

A total of 34 cases of HBV-related cirrhosis were selected for the study. All cases were surgically resected (lobectomy or explantation) for either HCC or end-stage liver cirrhosis. The patients ranged from 27 to 68 years (mean: 48 years) in age, and the male:female ratio was 2.4:1. The HBV-related etiology was confirmed by serological tests for HBsAg/HBeAg or evaluation of HBV DNA titers. Dysplastic nodules and HCCs were present in 11 (32.4%) and 21 (61.8%) cases, respectively. For comparison, non-neoplastic liver samples were obtained from 5 patients with metastatic colorectal carcinomas. All specimens were fixed in 10% formaldehyde, embedded in paraffin, and cut into 4  $\mu\text{m}$ -thick sections for routine hematoxylin-eosin staining, immunohistochemistry, TUNEL assay and quantitative fluorescent in situ hybridization (Q-FISH). For the SA- $\beta$ -Gal study, fresh frozen liver samples were obtained from 19 of the 34 cases of HBV-related cirrhosis.

### 2. Histological examination

On routine histological examination, all selected 34 cases demonstrated macronodular (21 cases) or mixed macro- and micronodular (13 cases) cirrhosis. The presence of LLCD and SLCD was determined according to previously described criteria: LLCD was defined as foci of hepatocytes showing cellular enlargement, nuclear pleomorphism, hyperchromasia and multinucleation, while SLCD was defined as foci of crowded small hepatocytes with high nuclear/cytoplasmic ratio.

### **3. Immunohistochemical stains for markers of cell cycle, proliferation and DNA damage**

Formalin-fixed paraffin-embedded tissues were sliced into 4 µm-thick sections, and immunohistochemistry was performed using the DAKO Envision Kit. In brief, sections were deparaffinized in xylene, rehydrated in graded alcohol and quenched in 3% hydrogen peroxidase. Antigen retrieval was performed in citrate buffer (pH6.0) in a 700W microwave oven for 15 minutes for p21, p27, p16, Tp53 and  $\gamma$ -H2AX, and with pepsin treatment for proliferating cell nuclear antigen (PCNA). The following primary antibodies were applied to the slides: p21 (p21<sup>WAF1/Cip1</sup>, clone SX118, 1:50, DAKO, Glostrup, Denmark), p27 (p27<sup>KIP1</sup>, clone SX53G8, 1:50, DAKO, Glostrup, Denmark), p16 (1:50, NeoMarkers, Fremont, CA, USA), Tp53 (clone DO-7, 1:50, DAKO, Glostrup, Denmark), PCNA (clone PC10, 1:50, DAKO, Glostrup, Denmark),  $\gamma$ -H2AX (1:100, Novus Biologicals, Littleton, CO, USA). Incubation was performed for 1 hour at room temperature. After rinsing, incubation with a secondary antibody was carried out using the DAKO EnVision Rabbit/Mouse kit (DAKO, Glostrup, Denmark), and then developed with 3,3-diaminobenzidine (DAKO, Glostrup, Denmark). Slides were then counterstained with hematoxylin, dehydrated, cleared and mounted. Dark brown nuclear staining was counted as positive for all antibodies, and the labeling indices (LI) were determined for each of these markers in non-dysplastic hepatocytes, LCD, SCD and HCC by dividing the number of positive nuclei under x400 magnification in at least five randomly selected fields by the total number of nuclei.

#### **4. Quantitative fluorescent in situ hybridization (Q-FISH) for telomere length**

Eighteen cases were subjected to Q-FISH study for telomere length. The peptide nucleic acid (PNA) probes used were as follows: Cy3-telomere probe (Applied Biosystems, Framingham, MA, USA) and FAM-centromere probe (5'-FAM-OO-ATTCGTTGGAAACGGGA-3'; Panagene, Daejeon, South Korea). 4 µm-thick formalin-fixed paraffin-embedded tissue sections were deparaffinized in xylene and rehydrated in graded alcohol. Antigen retrieval was performed in citrate buffer (pH6.0) in a 700W microwave oven for 10 minutes, and after washing, the sections were fixed in 10% buffered formalin. Treatment with protease I solution (1mg/ml, Vysis, Downers Grove, IL, USA) was performed at 37°C for 10 minutes, and sections were dehydrated in graded alcohol and air dried. The telomere/centromere probe mix (telomere: 2.5 µl 10 µg/ml PNA Cy3-telomere probe and 2.5 µl 25 µg/ml FAM-centromere probe) was applied to each section, followed by denaturation at 80°C for 3 minutes and hybridization at 37°C for 2 hours using Vysis HYBrite. Sections were washed in post-hybridization buffer (NP40/20xSSC, Vysis, Downers Grove, IL, USA) at room temperature for 30 minutes, followed by dehydration in graded alcohol, air drying and counterstaining with 5µl 4',6-diamidino-2-phenylindole (DAPI) I (Vysis, Downers Grove, IL, USA). Sections were viewed under a fluorescent microscope, and photographs were taken from each lesion under x1000 magnification at the following exposures: 1/100s for the DAPI images, and 1/3.5s for the Cy3 and FAM images. The telomere fluorescence intensity (TFI) and

centromere fluorescence intensity (CFI) signals were analyzed using the Image Pro Plus 5.0 software (MediaCybernetics, Silver Spring, MD, USA), and the mean ratio of telomere and centromere probes (TFI/CFI ratio) were calculated for each lesion.

### **5. Detection of apoptosis: transferase-mediated dUTP-biotin nick end labeling (TUNEL) assay**

Apoptosis detection was performed using the ApopTag Peroxidase In Situ Apoptosis Detection Kit (Chemicon International, USA), according to the manufacturer's instructions. Briefly, 4  $\mu\text{m}$ -thick formalin-fixed paraffin-embedded tissue sections were deparaffinized in xylene, rehydrated in graded alcohol and treated with protease I (20  $\mu\text{g}/\text{ml}$ ) at room temperature for 15 minutes. After quenching in 3% hydrogen peroxidase, 75  $\mu\text{l}$  of equilibrium buffer was applied to each section and sections were incubated at room temperature for 60 minutes. Subsequently, 55  $\mu\text{l}$  of TdT enzyme mix (70% reaction buffer, 30% TdT enzyme) was added to each section and incubated at 37°C for 60 minutes. After rinsing, staining was performed with anti-digoxigenin conjugate and 3,3-diaminobenzidine. Counterstaining was performed with 0.5% (w:v) methyl green, and slides were dehydrated, cleared and mounted. The TUNEL-labeling index (TUNEL-LI) was calculated as the number of positive nuclei under x400 magnification in at least five randomly selected fields by the total number of nuclei.

### **6. Senescence-associated $\beta$ -galactosidase (SA- $\beta$ -Gal) study**

Nineteen fresh frozen liver samples were cut into 6  $\mu\text{m}$ -thick sections and mounted onto glass slides. They were fixed with 2% glutaraldehyde and 3% formaldehyde for 3 to 5 minutes, followed by three washes in PBS at room temperature and incubated overnight at 37 with fresh SA- $\beta$ -Gal stain solution: 1 mg of 5-bromo-4-chloro-3-indolyl- $\beta$ -D-galactoside (X-Gal) per ml (stock: 20 mg/ml in dimethylformamide), in 49 mM citric acid, sodium phosphate, pH6.0, 5mM potassium ferrocyanide, 5 mM potassium ferricyanide, 150 mM NaCl, and 2 mM  $\text{MgCl}_2$ . After rinsing and counterstaining with nuclear fast red, slides were viewed under the light microscope. An accumulation of blue precipitate within the hepatocyte cytoplasm was regarded as evidence of SA- $\beta$ -Gal activity, and the number of hepatocytes with SA- $\beta$ -Gal activity was divided by the total number of hepatocytes in at least 5 high-power fields (x400 magnification) in each lesion to yield a percentage of hepatocytes with SA- $\beta$ -Gal activity. In addition, the intensity of SA- $\beta$ -Gal activity was also evaluated for each lesion and graded as weak (1+), moderate (2+) and strong (3+).

## **7. Micronuclei index**

Micronuclei of hepatocytes were identified by Feulgen-fast-green dyeing techniques. 4  $\mu\text{m}$ -thick formalin-fixed paraffin-embedded tissue sections were deparaffinized with xylene for 30 minutes, rehydrated with graded alcohol and then immersed in 0.1M hydrochloric acid at 60°C for 5 minutes. Slides were then immersed in Schiff reagent for 30 minutes until the nuclei were stained and were then transferred

directly to bisulphate water, followed by rinsing under running tap water. Counterstaining was performed with 0.1% fast green for 30 seconds.

The presence of micronuclei were defined using the following criteria: 1) a diameter smaller than one third of the nucleus; 2) micronuclei had to be non-refractive to be distinguished from artifacts such as small staining particles; 3) no connection to the main nuclei; 4) the same staining intensity as the main nuclei although occasionally staining may be more intense.<sup>38</sup> The hepatocytes with pyknotic nuclei or overlapping hepatocytes were not assessed for micronuclei count. The micronuclei index was calculated as the number of micronuclei per 1000 hepatocytes (‰).

## **8. Statistical analysis**

Statistical analysis was performed using the SPSS 15.0 software (SPSS Inc., Chicago, IL, USA). The Mann-Whitney U test was used to compare the results of the immunohistochemical studies, TUNEL assay, micronuclei index and quantitative FISH between the normal livers, non-dysplastic hepatocytes, LLCD, SLCD and HCC. A p-value of less than 0.05 was considered statistically significant for all analyses.

### III. RESULTS

#### 1. The prevalence of liver cell dysplasia in HBV-related cirrhosis

LLCD was found in 31 (91.2%) out of 34 patients with HBV-related cirrhosis, while SLCD was found in 19 (55.9%) out of the 34 cases (Figure 1). Although LLCD was diffusely scattered throughout the liver, LLCD foci were more prevalent in periseptal areas.

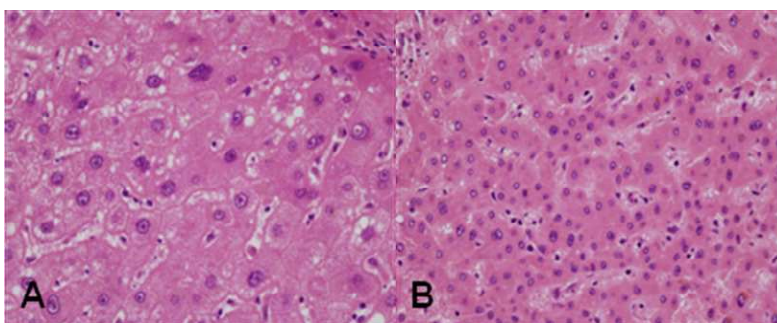


Figure 1. Histopathological features of liver cell dysplasia. (A) Large liver cell dysplasia (LLCD) is characterized by cellular enlargement, nuclear pleomorphism and hyperchromasia. (B) Small liver cell dysplasia (SLCD) demonstrates crowding of hepatocytes with high nuclear/cytoplasmic ratio.

#### 2. Cell cycle checkpoint markers in hepatocarcinogenesis

The LI of p21, p27 and p16 generally decreased from non-dysplastic hepatocytes, LLCD and SLCD, and increased slightly in HCC. More specifically, the p21-LI were 19.16%, 15.03%, 4.29% and 6.49% in average for non-dysplastic hepatocytes, LLCD, SLCD and HCC, respectively (Figures 2, 3). The difference in p21-LI were statistically significant between non-dysplastic hepatocytes and SLCD ( $p < 0.0001$ )

and HCC ( $p < 0.0001$ ) and between LLCDD and SLCD ( $p < 0.0001$ ) and HCC ( $p = 0.0001$ ). The p21-LI were lower in LLCDD compared to non-dysplastic hepatocytes, although not statistically significant ( $p = 0.060$ ). In normal livers, the p21-LI averaged 1.01% and there was a significant difference between normal livers and non-dysplastic hepatocytes ( $p < 0.001$ ).

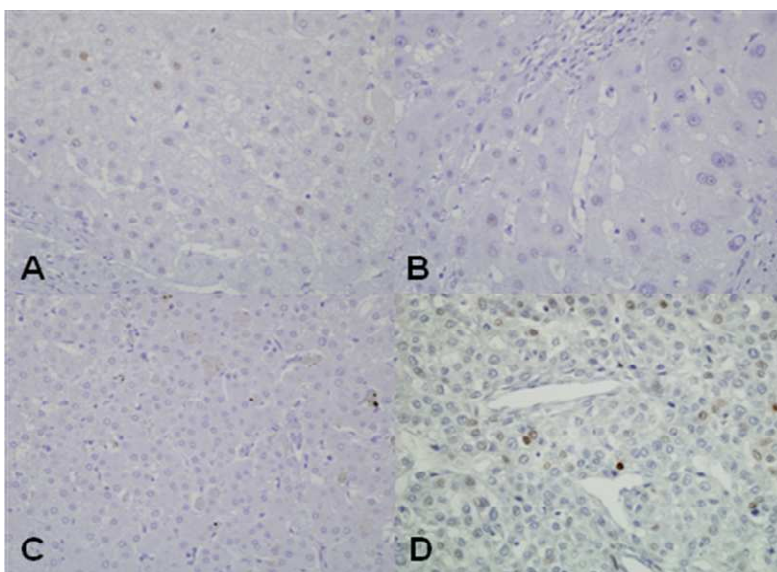


Figure 2. Immunohistochemical stain results for p21. The frequency of nuclear p21 expression is highest in non-dysplastic hepatocytes (A) and lower in LLCDD (B) and SLCD (C). The HCC showed the lowest p21 expression (D).

The p27 and p16-LI demonstrated similar patterns – 22.82%, 16.00%, 4.96% and 7.81% for p27 and 18.35%, 10.84%, 2.89% and 6.64% for p16 in non-dysplastic hepatocytes, LLCDD, SLCD and HCC foci, respectively (Figure 3). Statistically significant differences in p27 and p16-LI were found between non-dysplastic hepatocytes and LLCDD ( $p = 0.001$ ), SLCD ( $p < 0.001$ ) and HCC ( $p < 0.001$ ), between

LLCD and SLCD ( $p < 0.001$ ) and HCC ( $p = 0.002$  for p27 and  $p = 0.035$  for p16). As with the p21-LI, the difference between SLCD and HCC were not significant for both p27 and p16-LI. The p27 and p16-LI in normal livers averaged 1.09% and 0.84%, respectively.

Conversely, the expression of Tp53 increased from non-dysplastic hepatocytes, LLCD, SLCD and HCC: 1.36%, 9.49%, 13.87% and 45.24%, respectively (Figure 3). The difference in Tp53-LI were significant between non-dysplastic hepatocytes and LLCD ( $p < 0.001$ ), SLCD ( $p < 0.001$ ) and HCC ( $p < 0.001$ ), between LLCD and HCC ( $p = 0.001$ ), and between SLCD and HCC ( $p = 0.003$ ).

Table 1. Results of cell cycle checkpoint marker labeling index analysis (mean $\pm$ S.D, %)

	Ci	LLCD	SLCD	HCC
p21	19.16 $\pm$ 10.57	15.03 $\pm$ 10.86	4.29 $\pm$ 4.01	6.49 $\pm$ 9.57
p27	22.82 $\pm$ 6.01	16.00 $\pm$ 7.93	4.96 $\pm$ 3.11	7.81 $\pm$ 10.27
p16	18.35 $\pm$ 6.15	10.84 $\pm$ 5.71	2.89 $\pm$ 2.38	6.64 $\pm$ 10.11
Tp53	1.36 $\pm$ 1.81	9.49 $\pm$ 8.14	13.87 $\pm$ 11.87	45.24 $\pm$ 27.16

Ci: non-dysplastic hepatocytes, LLCD: large liver cell dysplasia, SLCD: small liver cell dysplasia, HCC: hepatocellular carcinoma

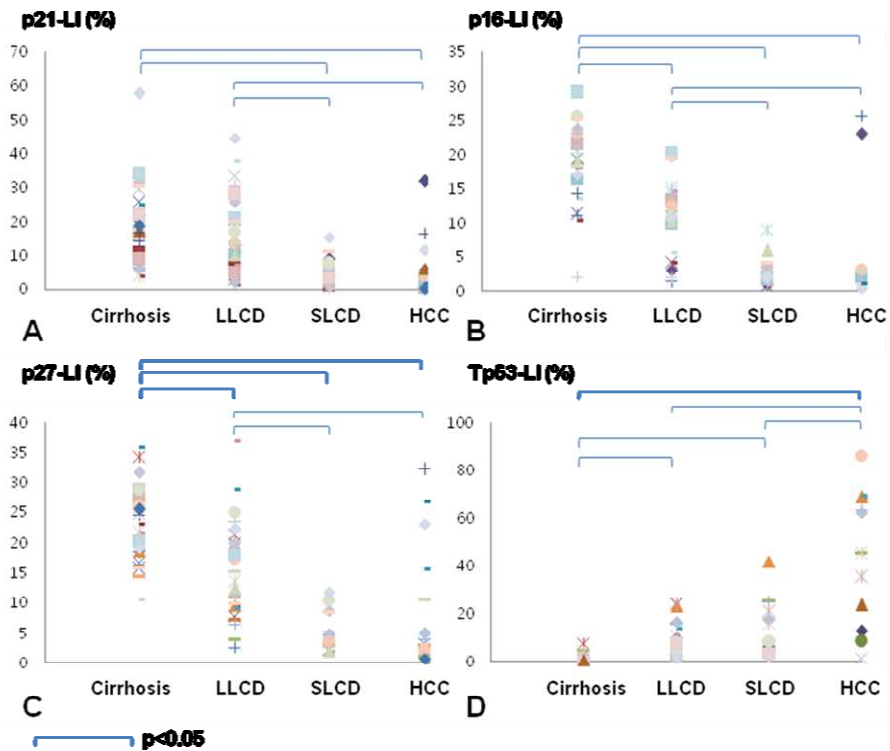


Figure 3. Scatter plots showing cell cycle checkpoint marker expression. There is a general decrease in the expression of p21 (A), p16 (B) and p27 (C), and an increase in the expression of mutant Tp53 protein (D) from non-dysplastic hepatocytes to LLCD, SLCD and HCC.

### 3. DNA damage markers in hepatocarcinogenesis

The  $\gamma$ -H2AX-LI averaged 23.12%, 45.74%, 59.21% and 82.94% in non-dysplastic hepatocytes, LLCD, SLCD and HCC, respectively, showing an increase in DNA damage foci (Figure 4, 5). The differences in  $\gamma$ -H2AX-LI were statistically significant between all lesions ( $p < 0.05$  for all). The micronuclei index was evaluated for 19 cases, and the average micronuclei indices were 0.24‰, 1.33‰,

2.65‰ and 9.67‰ for non-dysplastic hepatocytes, LLCD, SLCD and HCC, respectively (Figure 4, 5). There were statistically significant differences in the micronuclei index between all four lesions ( $p < 0.05$  for all). No micronuclei were found in normal livers.

Table 2. Results of  $\gamma$ -H2AX foci and micronuclei index analysis (mean $\pm$ S.D)

	Ci	LLCD	SLCD	HCC
$\gamma$ -H2AX (%)	23.12 $\pm$ 20.10	45.74 $\pm$ 30.66	59.21 $\pm$ 34.62	82.94 $\pm$ 21.13
Micronuclei (‰)	0.241 $\pm$ 0.703	1.330 $\pm$ 1.136	2.647 $\pm$ 0.927	9.669 $\pm$ 2.242

Ci: non-dysplastic hepatocytes, LLCD: large liver cell dysplasia, SLCD: small liver cell dysplasia, HCC: hepatocellular carcinoma

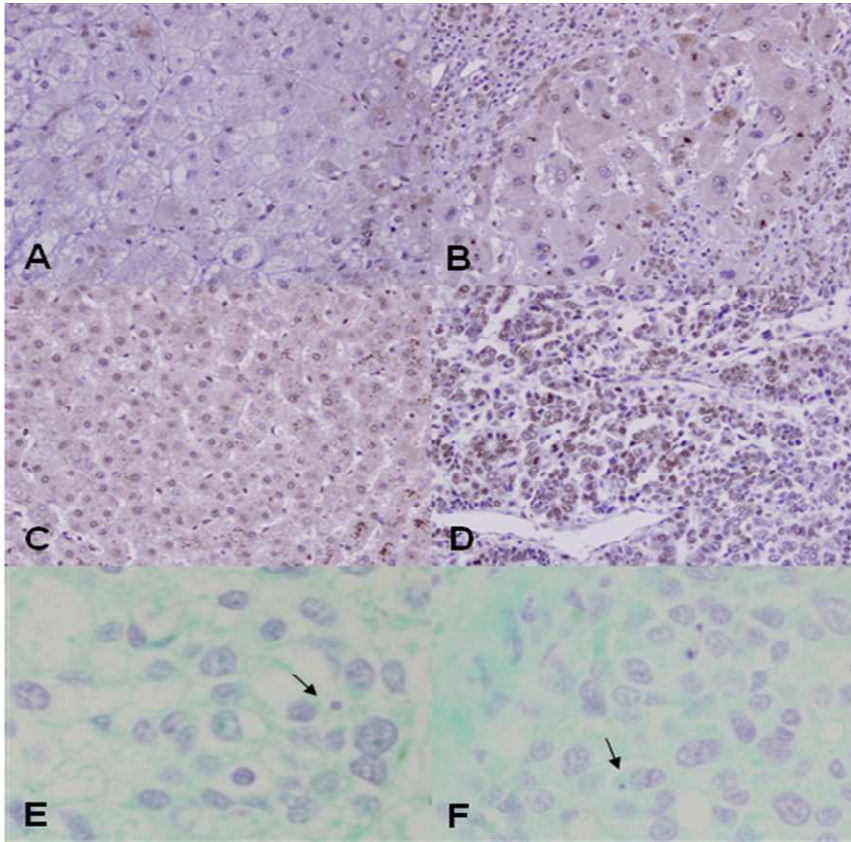


Figure 4. Immunohistochemical stain of  $\gamma$ H2AX foci (A-D) and micronuclei (E, F). The nuclear expression of  $\gamma$ H2AX increased significantly from non-dysplastic hepatocytes (A) to LLCD (B), SLCD (C) and HCC (D). Micronuclei in HCC are illustrated in (E, F), characterized by small masses of DNA in the cytoplasm resembling small nuclei recognizable by Feulgen stain.

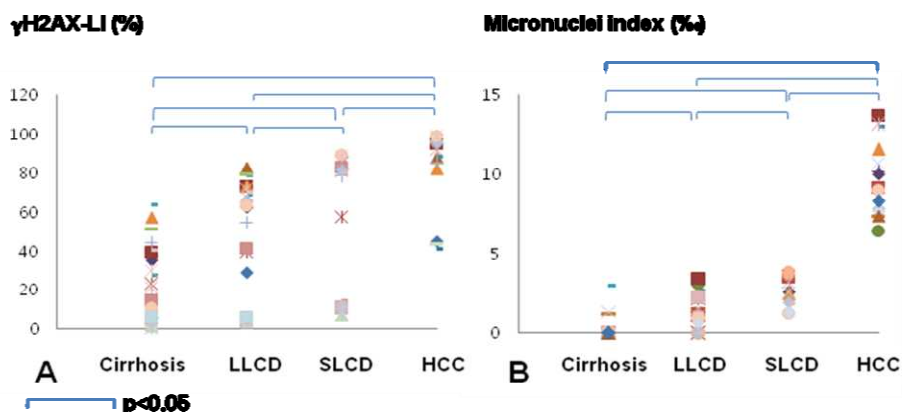


Figure 5. Scatter plots showing frequency of  $\gamma$ H2AX foci and micronuclei index. The level of DNA damage - demonstrated by the  $\gamma$ H2AX labeling index (%) (A) and the micronuclei index (%) (B) - increased significantly from non-dysplastic hepatocytes to LLCD, SLCD and HCC.

#### 4. Proliferation and apoptosis in hepatocarcinogenesis

The cell dynamics were studied, using the PCNA-LI and Ki-67-LI for proliferation and TUNEL-LI for apoptosis evaluation (Figure 6, Table 3). The PCNA-LI generally increased from non-dysplastic hepatocytes, LLCD, SLCD to HCC, averaging 5.28%, 12.42%, 15.61% and 46.45% for each lesion, respectively. Statistically significant differences were noted between non-dysplastic hepatocytes and LLCD ( $p=0.022$ ), SLCD ( $p=0.002$ ) and HCC ( $p<0.001$ ), between LLCD and HCC ( $p<0.001$ ) and between SLCD and HCC ( $p<0.001$ ). A similar pattern was seen with Ki-67-LI, although the labeling indices were lower as a whole: 0.32%, 1.18%, 4.43% and 14.17% in average for non-dysplastic hepatocytes, LLCD, SLCD and HCC, respectively. The Ki-67-LI was significantly higher in LLCD compared to

non-dysplastic hepatocytes ( $p=0.031$ ). Significant differences were also seen between non-dysplastic hepatocytes and SLCD ( $p<0.001$ ) and HCC ( $p<0.001$ ), and between LLCD and SLCD ( $p=0.038$ ) and HCC ( $p=0.008$ ). As for the apoptotic index, the TUNEL-LI averaged 1.28%, 0.51%, 0.65% and 1.70% for non-dysplastic hepatocytes, LLCD, SLCD and HCC, respectively, demonstrating a sharp decrease in apoptotic activity in LLCD from non-dysplastic hepatocytes, and an increase in HCC. The differences in apoptotic activity were significant for all lesions ( $p<0.05$ ), except for between LLCD and SLCD ( $p=0.343$ ) where the TUNEL-LI were similar. The net cellular gain was then calculated by subtracting TUNEL-LI from the proliferation index. When the TUNEL-LI was subtracted from the PCNA-LI, there was a significant increase in net cellular gain from non-dysplastic hepatocytes ( $3.48\pm 5.04\%$ ) to LLCD ( $10.77\pm 12.95\%$ ) ( $p=0.010$ ), and a marked increase in HCC reaching as high as 94.94% ( $44.85\pm 28.16\%$ ). However, the difference between LLCD and SLCD ( $12.24\pm 13.26\%$ ) was not statistically significant ( $p=0.305$ ). An increase in net cellular gain was also demonstrated by subtracting the TUNEL-LI from the Ki-67-LI:  $-1.05\pm 1.02\%$ ,  $0.80\pm 1.07\%$ ,  $2.63\pm 2.84\%$  and  $7.26\pm 8.31\%$  in non-dysplastic hepatocytes, LLCD, SLCD and HCC, respectively. Statistically significant differences were found between non-dysplastic hepatocytes and LLCD ( $p=0.001$ ), SLCD ( $p=0.003$ ) and HCC ( $p=0.001$ ). However, the differences between LLCD, SLCD and HCC failed to reach statistical significance.

Table 3. Results of proliferation and apoptosis index analysis (mean±S.D, %)

	Ci	LLCD	SLCD	HCC
PCNA	5.28±5.66	12.42±12.95	15.61±14.44	46.45±27.96
Ki-67	0.32±0.43	1.18±0.90	4.43±4.83	14.17±11.49
TUNEL	1.28±0.71	0.51±0.26	0.65±0.38	1.70±0.81
PCNA-TUNEL	3.48±5.04	10.77±12.95	12.24±13.26	44.85±28.16
Ki-67 - TUNEL	-1.05±1.02	0.80±1.07	2.63±2.84	7.26±8.31

Ci: non-dysplastic hepatocytes, LLCD: large liver cell dysplasia, SLCD: small liver cell dysplasia, HCC: hepatocellular carcinoma

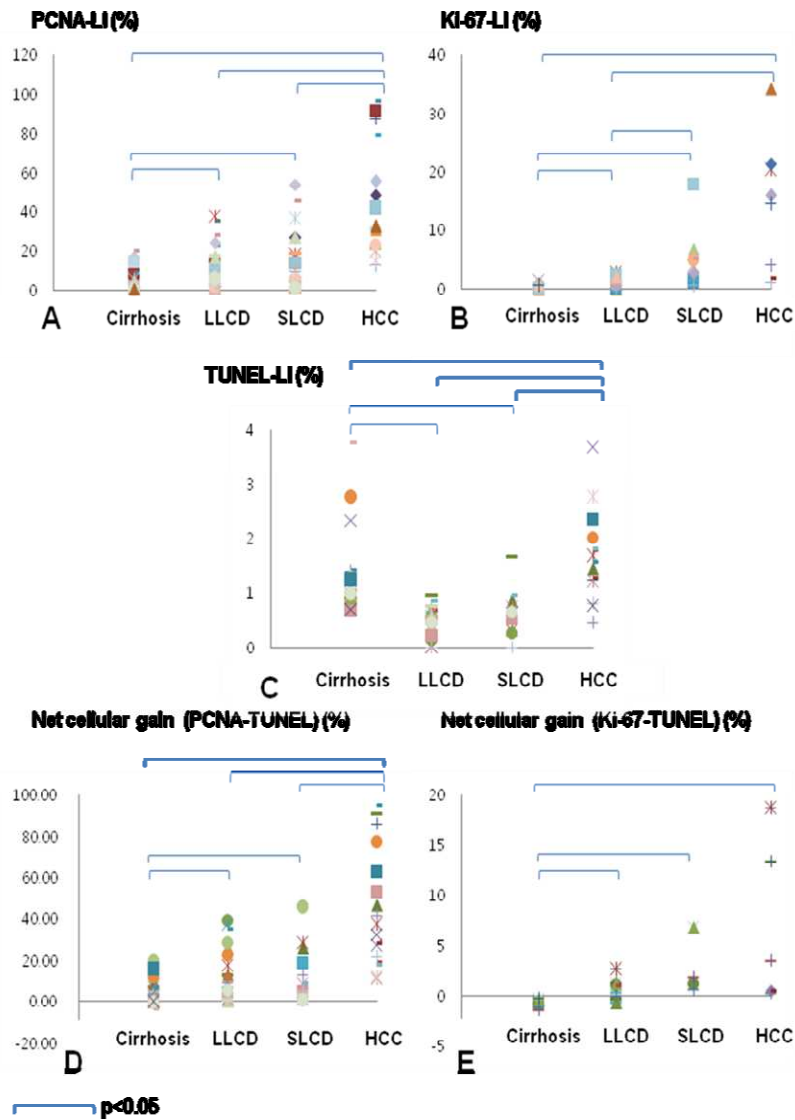


Figure 6. Scatter plots showing proliferation, apoptosis and net cellular gain. A remarkable increase in the PCNA-labeling index is seen from non-dysplastic hepatocytes to LLCD, SLCD and HCC (A). The apoptotic index (TUNEL-labeling index) decreases significantly in LLCD compared to non-dysplastic hepatocytes and shows an increase towards progression to HCC (B). The net cellular gain (PCNA-LI

– TUNEL-LI) is significantly increased during the progression from non-dysplastic hepatocytes to LLCD, SLCD and HCC (C).

### 5. Senescence markers in hepatocarcinogenesis

The telomere lengths were evaluated by quantitative FISH with the telomere PNA probe in 18 cases, and the mean telomere lengths for LLCD ( $p=0.001$ ), SLCD ( $p<0.001$ ) and HCC ( $p<0.001$ ) were all significantly shorter than hepatocytes in non-dysplastic hepatocytes (Figure 7). There was a gradual decrease in telomere length from non-dysplastic hepatocytes, LLCD, SLCD to HCC - 1.27, 1.07, 1.00 and 0.98 in average for each lesion respectively – however, the differences in telomere lengths between LLCD, SLCD and HCC failed to reach statistical significance. There was a significant shortening of telomere length in non-dysplastic hepatocytes compared to normal livers (mean: 1.532) ( $p=0.010$ ).

Table 4. Results of telomere length analysis (mean±S.D)

	Ci	LLCD	SLCD	HCC
TFI/CFI ratio	1.274±0.161	1.072±0.171	1.009±0.126	0.979±0.131

TFI: telomere fluorescent intensity; CFI: centromere fluorescent intensity; Ci: non-dysplastic hepatocytes, LLCD: large liver cell dysplasia, SLCD: small liver cell dysplasia, HCC: hepatocellular carcinoma

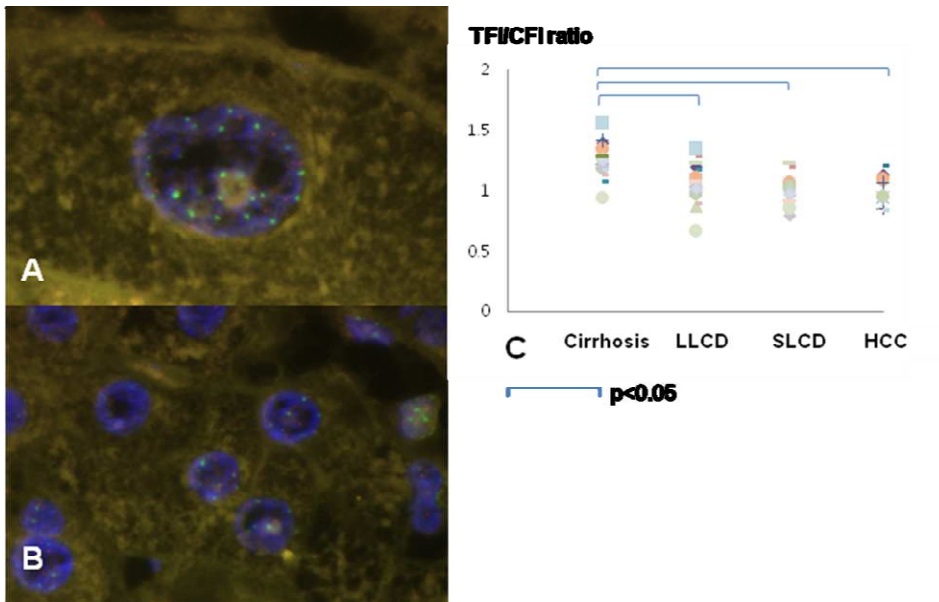


Figure 7. Results of quantitative FISH for telomere length assessment. The red (Cy3) and green (FAM) signals represent the telomere and centromere signals, respectively, in this example of LLCD (A) and SLCD (B). The telomere length was evaluated by calculating the telomere fluorescence intensity/centromere fluorescence intensity (TFI/CFI) ratio, and a significant decrease was found from non-dysplastic hepatocytes to LLCD, SLCD and HCC (D).

SA- $\beta$ -Gal activity was seen in periseptal hepatocytes in all 19 cirrhotic livers. The SA- $\beta$ -Gal-positive cells were counted in random fields, and the staining intensities were as follows: 3+ in one (5.3%), 2+ in 13 (68.4%) and 1+ in the remaining 5 (26.3%) cases. Two (11.8%) of 17 LLCD showed weak SA- $\beta$ -Gal activity, and SA- $\beta$ -Gal activity was absent in SLCD and HCC (Figure 8). The proportions of hepatocytes demonstrating SA- $\beta$ -Gal activity were as follows:  $26.09 \pm 17.25\%$ ,

0.58±1.62%, 0% and 0% in non-dysplastic hepatocytes, LLCD, SLCD and HCC, respectively (Table 5). There were significant differences in the SA- $\beta$ -Gal activity between non-dysplastic hepatocytes and LLCD ( $p<0.001$ ) and SLCD ( $p<0.001$ ) (Figure 9). SA- $\beta$ -Gal activity was not seen in normal livers.

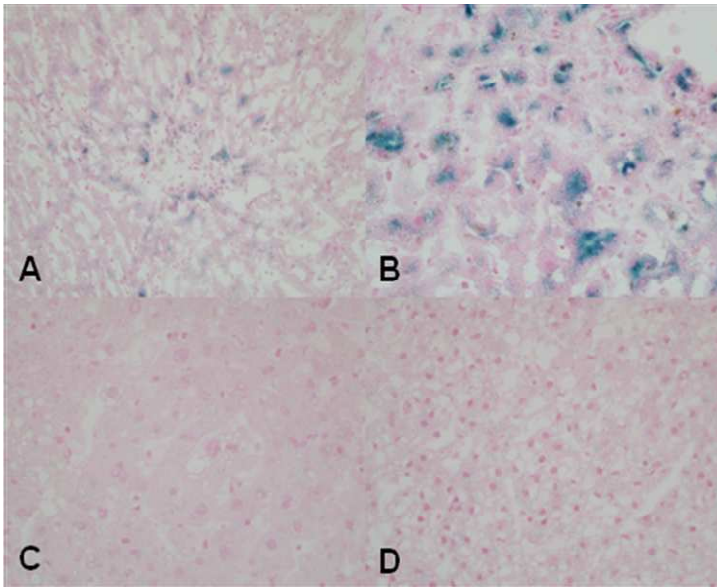


Figure 8. Results of senescence associated- $\beta$ -galactosidase (SA- $\beta$ -gal) study. Strong cytoplasmic staining is seen in non-dysplastic hepatocytes with a predominantly periseptal distribution (A, B). SA- $\beta$ -gal activity is not seen in LLCD (C) and in SLCD (D).

Table 5. Results of senescence-associated- $\beta$ -galactosidase activity analysis

(mean $\pm$ S.D, %)

	Ci	LLCD	SLCD	HCC
SA- $\beta$ -Gal	26.09 $\pm$ 17.25	0.58 $\pm$ 1.62	0	0

Ci: non-dysplastic hepatocytes, LLCD: large liver cell dysplasia, SLCD: small liver cell dysplasia, HCC: hepatocellular carcinoma

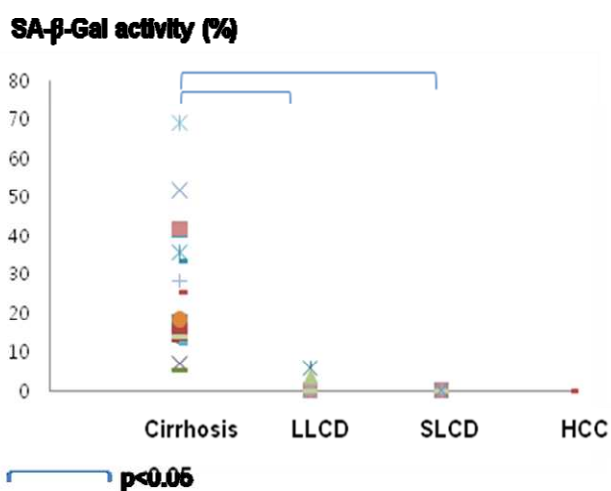


Figure 9. Scatter plots showing senescence associated- $\beta$ -galactosidase (SA- $\beta$ -gal) activity. A significant decrease in SA- $\beta$ -Gal activity is noted from non-dysplastic hepatocytes to LLCD and SLCD.

#### IV. DISCUSSION

Although LLCD is frequently found in cirrhosis and easily recognized even under low power magnification due to the characteristic cellular enlargement, nuclear pleomorphism, hyperchromasia and multinucleation, its presence is rarely reported by pathologists in practice and its significance is still under debate. While some results have favored a reactive/degenerative nature for the lesion,<sup>13,25,48</sup> there is increasing evidence that it may actually be related to hepatocarcinogenesis.<sup>9,11,14-16,18-24</sup> A comprehensive analysis of LLCD was performed in this study, evaluating various aspects of the lesion, including the cell cycle dynamics, proliferation and apoptosis, DNA damage and senescence.

The p21, p27 and p16 cell cycle checkpoint markers - which were expressed at low levels in normal hepatocytes - were activated in non-dysplastic hepatocytes but demonstrated increasing degrees of inactivation in LLCD, SLCD and HCC, along with an increase in mutant Tp53 protein expression. Plentz et al. previously reported that while the telomere was shortened in non-dysplastic hepatocytes and significant further shortening was noted in LLCD, SLCD and HCC, the cell cycle checkpoint marker, p21, was intact in LLCD, only to be inactivated in SLCD and HCC, implying that intact checkpoint responses may prevent proliferation of LLCD with shortened telomeres and prevent the evolution of DNA damage and chromosomal instability.<sup>49</sup> In this study, other cell cycle checkpoint markers, p27, p16 and Tp53 were also evaluated. p21, p53, p27 and p16 are all cell cycle regulators which have been shown to play a role in replicative senescence; p21 and p27 are components of the CIP/KIP pathway which are activated by p53 and TGF-  $\beta$ , respectively, and p16

is involved in the INK4a/ARF pathway.<sup>43</sup> Both pathways result in inactivation of cyclin-dependent kinases and subsequently cell cycle arrest at the G1-S transition.<sup>43</sup> Although there was only a tendency for a decrease in p21-LI in LLCD compared to non-dysplastic hepatocytes ( $p=0.060$ ), the p27 and p16-LI were significantly decreased, together with an increased expression of mutant Tp53 protein in LLCD, implying that cell cycle checkpoint responses may actually already be partly inactivated in LLCD.

The expression of Tp53 in LLCD is debatable. Only 3% of LLCD demonstrated mutant Tp53 protein expression in a study by Cohen et al. and the authors suggested that p53 mutation may be a late event in hepatocarcinogenesis.<sup>50</sup> Absence of Tp53 expression in LLCD was also shown by Zhao et al.<sup>51,52</sup> However, in this study the Tp53-LI was significantly increased in LLCD compared to non-dysplastic hepatocytes, ranging from 1.15% to 24.06% (mean  $\pm$  S.D.:  $9.49 \pm 8.14\%$ ) in LLCD, suggesting that more extensive studies with a greater number of cases may be required to further characterize the Tp53 overexpression status of LLCD.

In the study by Plentz et al., p21 and p16 inactivation was evident in SLCD and HCC, and it was speculated that the loss of cell cycle checkpoint markers may allow clonal expansion of hepatocytes with dysfunctional, shortened telomeres.<sup>49</sup> Similarly, a statistically significant difference in telomere length was seen between normal liver and non-dysplastic hepatocytes ( $p=0.010$ ), and between non-dysplastic hepatocytes and LLCD ( $p=0.001$ ) in this study. However, a significant difference in telomere length between LLCD, SLCD and HCC was not evident in the present study, although there was a general decrease from non-dysplastic hepatocytes,

LLCD, SLCD to HCC. A previous study by Oh et al. demonstrated that telomerase activity was significantly increased in high-grade dysplastic nodules and HCC compared to large regenerative nodules and low-grade dysplastic nodules, suggesting that telomerase reactivation and hence telomere stabilization occurs in high-grade dysplastic nodules.<sup>35</sup> Interestingly, the latter are characterized by dysplastic hepatocytes with morphological features of SLCD; therefore, telomerase reactivation may occur in SLCD and HCC, resulting in the absence of further significant telomere shortening in the two lesions.

As markers of DNA damage and chromosomal instability, the  $\gamma$ -H2AX-LI and the micronuclei index were evaluated. The accumulation of  $\gamma$ -H2AX foci and the micronuclei index were extremely low in normal hepatocytes and there was a significant gradual increase from non-dysplastic hepatocytes, LLCD, SLCD to HCC, again reflecting the increasing degree of DNA damage and chromosomal instability associated with loss of cell cycle checkpoints and dysfunctional telomeres in LLCD, SLCD and HCC.

LLCD may represent a “dead-end” of hepatocarcinogenesis – whether LLCD can progress to SLCD and subsequently to HCC remains to be determined.<sup>49</sup> Morphologically, it seems less likely that there is a transition between LLCD and SLCD/HCC. LLCD may actually represent cellular senescence in the context of a tumor suppressor mechanism preventing the proliferation of genetically unstable precancerous cells. Alternatively, oncogene-induced senescence, defined as the activation of oncogenes which induce a senescence checkpoint,<sup>41,42</sup> may be a possible mechanism for the formation of LLCD. Both suggestions point toward the

senescent nature of the lesion, that LLCD is a defensive mechanism against hepatocarcinogenesis. However, an increase in net cellular gain (high proliferative activity and low apoptotic index) from normal hepatocytes, non-dysplastic hepatocytes, LLCD, SLCD and HCC was seen in this study, similarly to a previous report by Koo et al.,<sup>21</sup> which may suggest that LLCD is not simply a quiescent senescent lesion, but actually is a proliferative one.

Although PCNA has been considered to be simply a marker of cell proliferation for decades, there is recent experimental evidence that PCNA actually has multiple roles including cell proliferation, DNA repair and cell cycle control. Two fractions of PCNA have been recognized in cycling cells: the detergent-soluble fraction and the detergent-insoluble/DNA-bound fraction, with the latter being the only one associated with DNA synthesis.<sup>53</sup> An increase in DNA-bound PCNA occurs during the S-phase, and PCNA relocates to repair sites together with p21 during DNA repair.<sup>54</sup> As there is at least some chromosomal instability and DNA damage in not only preneoplastic lesions but also in inflammatory conditions such as ulcerative colitis,<sup>55,56</sup> it may be argued that the PCNA-LI may not be an optimal marker that reflects cell proliferation alone. Furthermore, excess cyclin D1 has been demonstrated to bind to PCNA, resulting in the inhibition of DNA replication.<sup>57</sup> Therefore, in this study the Ki-67-LI was also studied, and although the sensitivity was strikingly lower compared to PCNA (e.g. Ki-67-LI in HCCs ranged from 1.07% to 34.18% while PCNA-LI ranged from 12.57% to 96.50%) a similar pattern of increasing proliferative activity and net cellular gain from non-dysplastic hepatocytes, LLCD, SLCD to HCC was observed. Additional novel sensitive

markers of proliferation such as minichromosome maintenance protein-2 (mcm-2) should be studied to further support the present data.<sup>58</sup>

Interestingly, the SA- $\beta$ -Gal activity was weaker and less frequent in LLCN compared to the periseptally located hepatocytes in non-dysplastic hepatocytes, which would be unexpected if LLCN represented a population of terminally differentiated end-stage hepatocytes. Contradictory results have been previously reported by Lee et al., showing a low proliferative rate and greater degree of apoptosis in their LLCN lesions compared to normal hepatocytes in cirrhotic livers of various etiologies.<sup>25</sup> However, although LLCN may be observed in various liver diseases such as autoimmune hepatitis, alcoholic cirrhosis and cholestatic liver, it has been reported to be more prevalent in HBV-associated chronic liver disease, ranging from 13-32% in studies of biopsied liver to 100% in studies of cirrhotic explanted livers, and it may be possible that the nature of LLCN depends on the biological setting where it arises.<sup>24,48,59-61</sup> For example, while LLCN in cholestatic liver may represent reactive change, in chronic viral hepatitis it might be preneoplastic.<sup>9</sup> This study, like the aforementioned studies by Koo et al.,<sup>21,22</sup> is focused on HBV-related cirrhosis. In fact, several prospective and retrospective studies have shown the presence of LLCN in needle biopsies of HBV-related chronic liver disease is an important independent risk factor for subsequent HCC development,<sup>22,24,62,63</sup> and together with the results of this present study, it may be suggested that LLCN in HBV-related chronic liver disease is not simply an innocent senescent lesion, but is indeed a preneoplastic lesion closely related to hepatocarcinogenesis.

## V. CONCLUSION

To characterize the nature of LLC<sub>D</sub>, various molecular features and cell dynamics of the lesion were evaluated and compared with non-dysplastic hepatocytes, SLCD and HCC to yield the following results:

1. The p21, p27 and p16 cell cycle checkpoint markers - which were expressed at low levels in normal hepatocytes - were activated in cirrhosis but were diminished gradually from LLC<sub>D</sub> through SLCD to HCC, along with an increase in mutant Tp53 protein expression.
2. Significant shortening of telomere length was seen in non-dysplastic hepatocytes compared to normal liver, and in LLC<sub>D</sub> compared to non-dysplastic hepatocytes. There was a general decrease in telomere length from non-dysplastic hepatocytes, LLC<sub>D</sub>, SLCD to HCC.
3. The accumulation of  $\gamma$ -H2AX foci and the micronuclei index were extremely low in normal hepatocytes and there was a significant gradual increase from non-dysplastic hepatocytes, LLC<sub>D</sub>, SLCD to HCC.
4. An increase in net cellular gain (high proliferative activity and low apoptotic index) from normal hepatocytes, non-dysplastic hepatocytes, LLC<sub>D</sub>, SLCD to HCC was seen.
5. The SA- $\beta$ -Gal activity was weaker and less frequent in LLC<sub>D</sub> compared to the periseptally located hepatocytes in non-dysplastic hepatocytes.

The increase in net cellular gain and the weak SA- $\beta$ -Gal activity in LLC<sub>D</sub> suggest that LLC<sub>D</sub> may represent a proliferative lesion rather than a population of terminally differentiated end-stage hepatocytes. The loss of cell cycle checkpoint

markers in LLCDC may allow clonal expansion of hepatocytes with dysfunctional, shortened telomeres, and accumulation of DNA damage and chromosomal instability.

## REFERENCES

1. Wada K, Kondo F, Kondo Y. Large regenerative nodules and dysplastic nodules in cirrhotic livers: a histopathologic study. *Hepatology* 1988;8:1684-8.
2. Sakamoto M, Hirohashi S, Shimosato Y. Early stages of multistep hepatocarcinogenesis: adenomatous hyperplasia and early hepatocellular carcinoma. *Hum Pathol* 1991;22:172-8.
3. Furuya K, Nakamura M, Yamamoto Y, Toge K, Otsuka H. Macroregenerative nodule of the liver. A clinicopathological study of 345 autopsy cases of chronic liver disease. *Cancer* 1988;61:99-105.
4. Theise ND, Schwartz M, Miller C, Thung SN. Macroregenerative nodules and hepatocellular carcinoma in forty-four sequential adult liver explants with cirrhosis. *Hepatology* 1992;16:949-55.
5. Ferrell L, Wright T, Lake J, Roberts J, Ascher N. Incidence and diagnostic features of macroregenerative nodules vs small hepatocellular carcinoma in cirrhotic livers. *Hepatology* 1992;16:1372-81.
6. Ferrell LD, Crawford JM, Dhillon AP, Scheuer PJ, Nakanuma Y. Proposal for standardized criteria for the diagnosis of benign, borderline and malignant hepatocellular lesions arising in chronic advanced liver disease. *Am J Surg Pathol*

1993;17:1113-23.

7. Hytioglou P, Park YN, Krinsky G, Theise ND. Hepatic precancerous lesions and small hepatocellular carcinoma. *Gastroenterol Clin N Am* 2007;36:867-87.

8. Crawford JM. Pathological assessment of liver cell dysplasia and benign liver tumors: differentiation from malignant tumors. *Semin Diagn Pathol* 1990;7:115-28.

9. Park YN, Roncalli M. Large liver cell dysplasia: a controversial entity. *J Hepatol* 2006;45:734-43.

10. Watanabe S, Okita K, Harada T, Kodama T, Numa Y, Takemoto T. Morphologic studies of the liver cell dysplasia. *Cancer* 1983;51:2197-205.

11. Anthony PP, Vogel CL, Barker LE. Liver cell dysplasia : a premalignant condition. *J Clin Pathol* 1973;26:217-23.

12. Libbrecht L, Desmet V, Roskams T. Preneoplastic lesions in human hepatocarcinogenesis. *Liver Int* 2005;25:16-27.

13. Marchio A, Terris B, Meddeb M, Pineau P, Duverger A, Tiollais P et al. Chromosomal abnormalities in liver cell dysplasia detected by comparative genomic hybridization. *Mol Pathol* 2001;54:270-4.

14. Roncalli M, Borzio M, Brando M, Colloredo G, Servida E. Abnormal DNA content in liver cell dysplasia: a flow cytometric study. *Int J Cancer* 1989;44:204-7.
15. Thomas RM, Berman JJ, Yetter RA, Moore GW, Hutchins GM. Liver cell dysplasia: a DNA aneuploid lesion with distinct morphologic features. *Hum Pathol* 1992;23:496-503.
16. Orsatti G, Theise ND, Thung SN, Paronetto F. DNA image cytometric analysis of macroregenerative nodules (adenomatous hyperplasia) of the liver: evidence in support of their preneoplastic nature. *Hepatology* 1993;17:621-7.
17. Rubin EM, DeRose PB, Cohen C. Comparative image cytometric DNA ploidy of liver cell dysplasia and hepatocellular carcinoma. *Mod Pathol* 1994;7:677-80.
18. El-Sayed SS, El-Sadany M, Tabll AA, Soltan A, El-Dosoky I, Attallah AS. DNA ploidy and liver cell dysplasia in liver biopsies from patients with liver cirrhosis. *Can J Gastroenterol* 2004;18:87-91.
19. Zondervan PE, Wink J, Alers JC, Ijzermans JN, Schalm SW, de Man RA et al. Molecular cytogenetic evaluation of virus-associated and non-viral hepatocellular carcinoma: analysis of 26 carcinomas and 12 concurrent dysplasias. *J Pathol* 2000;192:207-15.

20. Terris B, Ingster O, Rubbia L, Dubois S, Belghiti J, Feldmann G et al. Interphase cytogenetic analysis reveals numerical chromosome aberrations in large liver cell dysplasia. *J Hepatol* 1997;27:313-9.
21. Koo JS, Seong JK, Park C, Yu DY, Oh BK, Oh SH et al. Large liver cell dysplasia in hepatitis B virus X transgenic mouse liver and human chronic hepatitis B virus-infected liver. *Intervirology* 2005;48:16-22.
22. Paradis V, Laurendeau I, Vidaud M, Bedossa P. Clonal analysis of macronodules in cirrhosis. *Hepatology* 1998;28:953-8.
23. Koo JS, Kim H, Park BK, Han KH, Chon CY, Park C et al. Predictive value of liver cell dysplasia for development of hepatocellular carcinoma in patients with B-viral hepatitis. *J Clin Gastroenterol* 2008 Feb [Epub ahead of print].
24. Libbrecht L, Craninx M, Nevens F, Desmet V, Roskams T. Predictive value of liver cell dysplasia for development of hepatocellular carcinoma in patients with non-cirrhotic and cirrhotic chronic viral hepatitis. *Histopathology* 2001;39:66-73.
25. Lee RG, Tsamandas AC, Demetris AJ. Large cell change (liver cell dysplasia) and hepatocellular carcinoma in cirrhosis: matched case-control study, pathological analysis, and pathogenetic hypothesis. *Hepatology* 1997;26:1415-22.

26. Ishikawa F. Telomere crisis, the driving force in cancer cell evolution. *Biochem Biophys Res Comm* 1997;230:1-6.
27. Linger J, Cech TR. Telomerase and chromosome end maintenance. *Curr Opin Genet Dev* 1998;8:226-32.
28. di Fagagna FA, Teo SH, Jackson SP. Functional links between telomeres and proteins of the DNA-damage response. *Genes Dev* 2004;18:1781-99.
29. Deng Y, Chang S. Role of telomeres and telomerase in genomic instability, senescence and cancer. *Lab Invest* 2007;87:1071-6.
30. Gisselsson D, Hoglund M. Connecting mitotic instability and chromosome aberrations in cancer – can telomeres bridge the gap? *Sem Cancer Biol* 2005;15:13-23.
31. Ozturk N, Erdal E, Mumcuoglu M, Alcali KC, Yalcin O, Senturk S et al. Reprogramming of replicative senescence in hepatocellular carcinoma-derived cells. *Proc Natl Acad Sci USA* 2006;103:2178-83.
32. Shay JW, Roninson IB. Hallmarks of senescence in carcinogenesis and cancer therapy. *Oncogene* 2004;23:2919-33.

33. Plentz RR, Caselitz M, Bleck JS, Gebel M, Flemming P, Kubicka S et al. Hepatocellular telomere shortening correlates with chromosomal instability and the development of human hepatoma. *Hepatology* 2004;40:80-6.
34. Plentz RR, Schlegelberger B, Flemming P, Gebel M, Kreipe M, Manns MP et al. Telomere shortening correlates with increasing aneuploidy of chromosome 8 in human hepatocellular carcinoma. *Hepatology* 2005;42:522-6.
35. Oh BK, Chae KJ, Park C, Kim K, Lee WJ, Han KH et al. Telomere shortening and telomerase reactivation in dysplastic nodules of human hepatocarcinogenesis. *J Hepatol* 2003;39:786-92.
36. Oh BK, Kim H, Park YN, Yoo JE, Choi J, Kim KS et al. High telomerase activity and long telomeres in advanced hepatocellular carcinomas with poor prognosis. *Lab Invest* 2008;88:144-52.
37. Fenech M. The in vitro micronucleus technique. *Mutation Res* 2000;455:81-95.
38. de Almeida TMB, Leitao RC, Andrade JD, Becak W, Carrilho FJ, Sonohara S. Detection of micronuclei formation and nuclear anomalies in regenerative nodules of human cirrhotic livers and relationship to hepatocellular carcinoma. *Cancer Genet Cytogenet* 2004;150:16-21.

39. Sharpless NE, DePinho RA. Crime and punishment. *Nature* 2005;436:636-7.
40. te Poele RH, Okorokov AL, Jardine L, Cummings J, Joel SP. DNA damage is able to induce senescence in tumor cells in vitro and in vivo. *Cancer Res* 2002;62:1876-83.
41. Collado M, Serrano M. The power and the promise of oncogene-induced senescence markers. *Nature Rev* 2006;6:472-6.
42. Collado M, Gil J, Efeyan A, Guerra C, Schuhmacher AJ, Barradas M et al. Tumour biology : senescence in premalignant tumours. *Nature* 2005;436:642.
43. Morgan DO. The cell cycle control system. In: Morgan DO. *The cell cycle: Principles of control*. Oxford University Press; 2007. p.28-55.
44. Quereda V, Martinalbo J, Dubus P, Carnero A, Malumbres M. Genetic cooperation between p21<sup>CIP1</sup> and INK4 inhibitors in cellular senescence and tumor suppression. *Oncogene* 2007;26:7665-74.
45. Dimri GP, Lee X, Basile G, Acosta M, Scott G, Roskelley C et al. A biomarker that identifies senescent human cells in culture and in aging skin in vivo. *Proc Natl Acad Sci USA* 1995;92:363-7.

46. Paradis V, Youssef N, Dargere D, Ba N, Bonvoust F, Deschatrette J et al. Replicative senescence in normal liver, chronic hepatitis C, and hepatocellular carcinomas. *Hum Pathol* 2001;32:327-32.
47. Satyanarayana A, Greenberg RA, Schaezlein S, Buer J, Masutomi K, Hahn WC et al. Mitogen stimulation cooperates with telomere shortening to activate DNA damage responses and senescence signaling. *Mol Cell Biol* 2004;24:5459-74.
48. Natarajan S, Theise ND, Thung SN, Antonio L, Paronetto F, Hytioglou P. Large-cell change of hepatocytes in cirrhosis may represent a reaction to prolonged cholestasis. *Am J Surg Pathol* 1997;21:312-8.
49. Plentz RR, Park YN, Lechel A, Kim H, Nellessen F, Langkopf BHE et al. Telomere shortening and inactivation of cell cycle checkpoints characterize human hepatocarcinogenesis. *Hepatology* 2007;45:968-76.
50. Cohen C, DeRose PB. Immunohistochemical p53 in hepatocellular carcinoma and liver cell dysplasia. *Mod Pathol* 1994;7:536-9.
51. Zhao M, Zhang N-X, Laissue JA, Zimmermann A. Immunohistochemical analysis of p53 protein overexpression in liver cell dysplasia and in hepatocellular carcinoma. *Virchows Archiv* 1994;424:613-21.

52. Zhao M, Zimmermann A. Apoptosis in human hepatocellular carcinoma and in liver cell dysplasia is correlated with p53 protein immunoreactivity. *J Clin Pathol* 1997;50:394-400.

53. Bravo R, Macdonald-Bravo H. Existence of two populations of cyclin/proliferating nuclear cell antigen during the cell cycle: association with DNA replication sites. *J Cell Biol* 1987;105:1549-54.

54. Gramantieri L, Trere D, Chieco P, Lacchini M, Giovannini C, Piscaglia F et al. In human hepatocellular carcinoma in cirrhosis, proliferating cell nuclear antigen (PCNA) is involved in cell proliferation and cooperates with p21 in DNA repair. *J Hepatol* 2003;39:997-1003.

55. Rabinovitch PS, Dziadon S, Brentnall TA et al. Pancolonial chromosomal instability precedes dysplasia and cancer in ulcerative colitis. *Cancer Res* 1999;59:5148-53.

56. Hermsen M, Postma C, Baak J et al. Colorectal adenoma to carcinoma progression follows multiple pathways of chromosomal instability. *Gastroenterology* 2002;123:1109-19.

57. Fukami-Kobayashi J, Mitsui Y. Cyclin D1 inhibits cell proliferation through

binding to PCNA and cdk2. *Exp Cell Res* 1999;246:338-47.

58. Freeman A, Hamid S, Morris L, Vowler S, Rushbrook S, Wight DGD et al. Improved detection of hepatocyte proliferation using antibody to the pre-replication complex: an association with hepatic fibrosis and viral replication in chronic hepatitis C virus infection. *J Viral Hepatitis* 2003;10:345-50.

59. Hytioglou P, Theise ND, Schwartz M, Mor E, Miller C, Thung SN. Macroregenerative nodules in a series of adult cirrhotic liver explants: issues of classification and nomenclature. *Hepatology* 1995; 21: 703-8.

60. Le Bail B, Bernard PH, Carles J, Balabaud C, Bioulac-Sage P. Prevalence of liver cell dysplasia and association with HCC in series of 100 cirrhotic liver explants. *J Hepatol* 1997;27:835-42.

61. Lefkowitz JH, Schiff ER, Davis GL, Perrillo RP, Lindsay K, Bodenheimer Jr HC et al. Pathological diagnosis of chronic hepatitis C: a multicenter comparative study with chronic hepatitis B. *Gastroenterology* 1993;104:595-603.

62. Borzio M, Bruno S, Roncalli M, Mels GC, Ramella G, Borzio F et al. Liver cell dysplasia is a major risk factor for hepatocellular carcinoma in cirrhosis: a prospective study. *Gastroenterology* 1995;108:812-7.

63. Ganne-Carrie N, Chastang C, Chapel F, Munz C, Pateron D, Sibony M et al. Predictive score for the development of hepatocellular carcinoma and additional value of liver large cell dysplasia in Western patients with cirrhosis. *Hepatology* 1996;23:1112-8.

< ABSTRACT (IN KOREAN)>

만성 B형 간염 바이러스성 간질환에서 큰 간세포 이형성의 의의

<지도교수 박 영 년>

연세대학교 대학원 의학과

김 혜 령

간세포 이형성은 육안적으로 확인할 수 없는 1mm 이하의 크기의 병변으로 뚜렷한 결절을 형성하지 않으며 작은 간세포 이형성 (small liver cell dysplasia; SLCD)와 큰 간세포 이형성 (large liver cell dysplasia; LLCDC)으로 분류할 수 있다. SLCD는 전암병변으로서 어느 정도 개념이 정립되어 있으나, LLCDC의 경우는 단순한 반응성 변화인지, 또는 간세포암종 발생과 밀접한 연관이 있는 전암병변인지 아직 의견의 일치가 없다. 본 연구에서는 LLCDC의 유전생물학적 특성에 대하여 살펴보고 LLCDC의 전암병변으로서의 의의를 밝히는 것이 목적이다.

외과적으로 절제한 만성 B형 간염 바이러스성 간경변 34 증례를 대상으로 연구를 시행하였으며 LLCDC 31증례, SLCD 19증례 및 HCC 21증례가 포함되었다. 세포주기조절인자인 p21, p27, p16, Tp53, DNA 손상 표지자인  $\gamma$ -H2AX에 대한 면역조직화학염색을 시행하였고, 세

포역동성을 알아보기 위하여 세포증식능 표지자 PCNA와 Ki-67 발현을 및 세포고사의 빈도를 측정하였다. 또한 Feulgen 방법으로 미세핵의 빈도를 구하여 염색체 불안정성의 정도를 살펴보고, 정량적인 형광제자리부합화 방법으로 각 병변세포의 텔로미어 길이를 측정하였으며, senescence-associated  $\beta$ -galactosidase (SA- $\beta$ -Gal) 염색으로 세포노화 여부를 판단하였다.

이형성이 없는 간세포, LLC<sub>2</sub>, SLCD 및 간세포암종의 순서로 세포주기조절인자 (p21, p27, p16, p53)의 소실의 정도가 높았고,  $\gamma$ -H2AX 병소 및 미세핵의 빈도도 점점 증가하는 양상을 보였다. PCNA, Ki-67 및 TUNEL labeling index로 알아본 net cellular gain도 이형성이 없는 간세포, LLC<sub>2</sub>, SLCD, 간세포암종 순으로 높아졌으며, 텔로미어 길이는 점점 짧아졌고, SA- $\beta$ -Gal 염색상 간경변에서는 노화된 세포가 많이 관찰되었으나, LLC<sub>2</sub> 및 SLCD에서는 관찰되지 않았다. 따라서 LLC<sub>2</sub>는 노화성 병변보다는 증식성 병변일 가능성이 더 높을 것으로 판단되며, 세포주기조절인자의 비활성화, 텔로미어 길이의 감소, DNA 손상 및 염색체 불안정성의 증가를 보이는 병변으로 간암발생과 밀접한 연관이 있는 전암병변일 가능성을 본 연구에서 제시하고자 한다.

---

핵심되는 말: 큰 간세포 이형성, 간세포암종, B형 간염 바이러스